# DESIGN CONSIDERATIONS FOR A LAMBERTSON SEPTUM MAGNET FOR THE SPALLATION NEUTRON SOURCE *

J. Rank, K. Malm, G. Miglionico, D. Raparia, N. Tsoupas, J. Tuozzolo, Y.Y. Lee
Collider-Accelerator Department, Brookhaven National Laboratory, Upton, NY 11973, USA

## Abstract

Multiple-stage injections to an accumulator ring boost intensity until a final extraction delivers the full proton beam to a target transfer line. Kickers and an Extraction Lambertson Septum (ELS) magnet implement extraction.

Studied here are various concerns of the design of an ELS magnet, including: lattice geometry, beam dynamics and optics considerations; and vacuum, electromagnetic and mechanical design aspects. Reference datum and transformations are established and shown schematically. Coil, yoke, and shield design optimization is discussed.

## 1 INTRODUCTION

A Lambertson Septum Magnet intercepts and redirects the proton beam of the accumulator ring toward the target on extraction cycles, yet passes undisturbed the ring's circulating beam on accumulation cycles. The Extraction Region (ER), in a straight section of the accumulator ring (Fig. 1), consists of consecutively: A set of pulsed Kickers [1], each of which bump the beam at a downward "kick angle" in a vertical plane; the subject Lambertson Septum magnet; and finally the Quadrupole Doublets which refocus and correct beam projection to target.
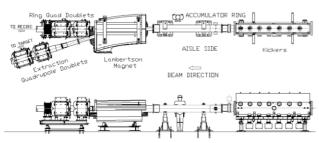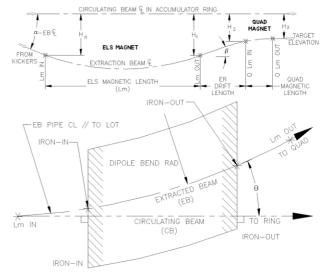


Figure 1: SNS Extraction Region plan and elevation views.

## 2 DESIGN CRITERIA

ELS design must satisfy constraints of the ER lattice specification: That the intercepted beam entering at the kicked angle ($a_{EB\ CL}$) finally exit to the transfer line on a path lying in a horizontal plane at the established target elevation (Fig. 2), and at an exit angle ($Q$) relative to the ring dictated by the lattice to-target projection (Fig. 3). To satisfy these, specifically for SNS with a committed target elevation, by design beam center is displaced vertically from magnet center at the first quadrupole; this introduces a small dipole component that corrects for a slight angular offset from the horizontal ($b$).

To avoid error magnification in 400 circulation passes per extraction cycle, we optimize electromagnetics for the circulating beam in the ring (CB). To this end, at beam



Figures 2 & 3: ER elevation (top) and plan view schematics.

entrance and exit, yoke design includes: iron squared to CB path, not the extracted beam (EB) path, to minimize quadrupole affects on CB; and allowance of space for "porch shielding" of the CB beyond the fringe field by tightening the bend radius to shorten iron length. Provision is also made to capture the CB within a shield assembly consisting of the "septum plate" and the "shield plate" (Fig.4). Between these plates "clamshells" the CB vacuum chamber wrapped in a thin non-magnetic copper shim to provide an effective impedance to flux to which the CB would be exposed. A narrow "shield cap" runs along CB axis, flush with the shield assembly. Total iron thickness (minus CB pipe OD) yields a flux density within iron saturation limits, even with inner-outer return path asymmetry as CB moves outboard of ELS center. Though ELS cross-section has near symmetry at the entrance saturation concerns persist in the thin septum.
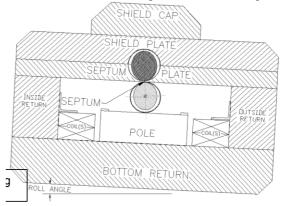


Figure 4: World x-y plane section at beam entrance to yoke.

## 3 OPTICS AND GEOMETRY

Of four SNS operating modes, ELS design is based on physics parameters for the largest beams. In all modes the elliptical beam sections of both CB and EB diverge along both major and minor axes (y and x, respectively). The y-axis divergence of the EB, and the known kick angle of the EB centerline, ultimately determine ELS magnetic geometry. To maximize septum thickness each vacuum pipe remains always tangent to the major axes of the beam it contains; i.e., CB and EB points-of-tangency (POT) occur at 6 and 12 o'clock orientations respectively (Fig. 5). Thus pole (magnet yoke) geometry must be everywhere parallel to the EB pipe centerline. This pipes diameter is determined by the EB size at the exit, and thus fixes the magnetic gap; the distance between the primary pole and the septum quasi-pole (Fig. 6). Similarly, there exists an angular offset of the CB with respect to its vacuum pipe which determines the axis of the cut hole in the shield assembly. These angular offsets are corrected at both exit flanges with "skewed" bores which center the beam path in the downstream pipe. Bore angles are offset also at the upstream "crotched" entrance flange. The shim "air gap" runs the length of the magnet including shielding porches, but terminates at the "field clamp". The clamp, in contact with the magnetic CB pipe, closes the electromagnetic circuit at end of air gap for stray flux.



Figure 5: Schematic of world x-y section at beam entrance.
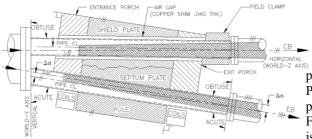


Figure 6: Schematic of world x-z section through pipe centers.

Recalling ELS design criteria, entering beam kicked downward relative to a world horizontal plane (WCS x-z) exits in that plane at a lattice-prescribed height and angle. Thus yoke geometry cannot be orthogonal to *any* WCS axis; i.e., the plane-of-pole (POP) first must lie tangent to an axis pitched about the world-x in order to receive the entering kicked beam, and second must be rolled about that pitch-axis in order to project the exiting beam at the given extracted angle, but parallel to the WCS x-z plane (or nearly; section 2). To gain pipe-to-diverging-beam tangency, pipe rotation about the world-x is by the kick angle ($a_{EB\,CL}$) less the EB y-radii divergence angle ($Da$).

$$\overline{V_{pop}} := \left(\overline{V_{wcs}}\cdot[T_{pitch}]\right)\cdot[T_{roll}] \ \text{where} \ \overline{V_{pop}} := \left(V''_x \ V''_y \ V''_z\right) \ \text{thus}$$

$$\frac{V''_x}{V_{wcs}} := \left[\sin(\gamma)\cdot\left[\frac{\tan(\theta)}{\tan(\gamma)} + \sin(\alpha)\cdot\left(1 - \frac{\tan(\beta)}{\tan(\alpha)\cdot\cos(\theta)}\right)\right]\right]$$

$$\frac{V''_y}{V_{wcs}} := \left[\cos(\gamma)\cdot\left[\tan(\gamma)\cdot\tan(\theta) - \sin(\alpha)\cdot\left(1 - \frac{\tan(\beta)}{\tan(\alpha)\cdot\cos(\theta)}\right)\right]\right]$$

$$\frac{V''_z}{V_{wcs}} := \left[\cos(\alpha)\cdot\left(1 + \frac{\tan(\alpha)\cdot\tan(\beta)}{\cos(\theta)}\right)\right] \ \text{where} \ \begin{array}{l}\alpha \ \text{is pitch angle}\\ \gamma \ \text{is roll angle}\end{array}$$

Given $(V''_x)^2 + (V''_z)^2 := V_{wcs}$ and $V''_y := 0$ solve for $\alpha, \gamma$

Figure 7: POP to WCS coordinate transformation.

To relate ELS pole coordinate system (POP CS) to the customary perspective for a conventional dipole in the WCS, one must perform a series of two coordinate transformations. Mathematically, the matrix algebra of Fig. 7 is solved for both the divergence-corrected pitch angle ($a_{LOT}$) and the roll angle ($g$) given constraints on lattice geometry ($b$ & $Q$ of Fig. 2 & 3). Visually, we first rotate the viewing direction in Fig. 5 by the corrected pitch angle (Fig. 8), then by the roll angle (Fig. 9).
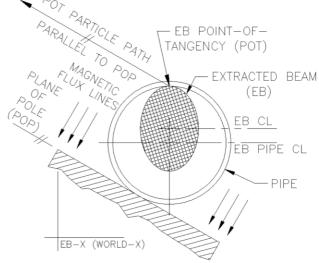


Figure 8: Pitch-corrected view of EB and pole.

We may resolve the velocity vector *v* of an arbitrary particle entering ELS field into components orthogonal to POP; i.e., aligned with the flux lines (POP-y axis, perpendicular to the pole), or lying in the POP (POP x-z). Fig. 10 depicts a particle on the LOT path. The vector *v* is resolved into components orthogonal to the POP CS. The resultant of vectors parallel to the POP is *v // POP*.
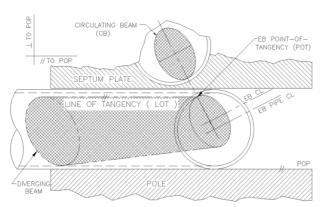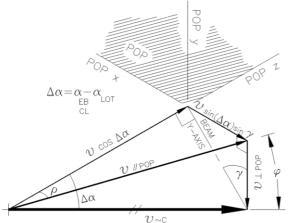
Figure 9:  POP x-y plane section schematic at beam entrance.

Bend radius due to ELS field is proportional to ***v // POP*** ; but the component perpendicular to POP remains constant along the particle path.  Thus only a particle positioned at the EB POT will travel on a circular arc always parallel to the POP; this line-of-tangency (LOT) arc shows in Fig. 9. All others, including those on beam center, have constant non-zero POP-y velocity component.  Hence, the EB path through the ELS is a helix; the particle bunch appears as a "horn on a table" in contact on its LOT.  This adds subtle complexities to 3D model development, lattice placement, and specification of survey and alignment at installation. A datum point used to place a conventional dipole, where entering and exiting centerlines intersect, does not exist.
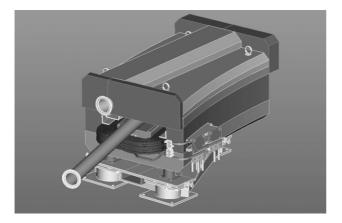


Figure 10: Velocity vector POP components for LOT particle.



Figure 11:  ELS magnet assembly view looking upstream.

## 4  ELS MAGNET ASSEMBLY

A discussion of design issues for the various components of the ELS magnet assembly (Fig. 11) is useful.

### Coils

Water-cooled coils, sized for 1.3 GeV, have the following specifications: Allowable $20^0$C rise, 70 psid max, 5-15 fps turbulent flow, and current density <1000 A/sq. cm. [2]. The resulting large cooling passage raises concerns about intermediate splice design, and "keystoning" at the bends. Radiation exposure of septa warrant "rad-hard" coils.

### Vacuum Chamber

Chamber manufacture requires many stages. The CB pipe from ASTM A513 DOM tube for dimensional accuracy, is placed in an acid bath, vacuum fired, masked at the weld joints, and nickel plated inside and out.  The tube is welded to 304L flanges of the now-formed EB weldment, including the delicate weld at the crotch.  Care is taken here as the weld is compounded by: a thin base metal, a tight fit, dissimilar metals, a fragile nickel plating, and high stresses.  Finally, the tube is TiN coated.

### Shielding and Yoke

Kicker design limits septum thickness; as weighed against competing concerns of saturation and stress.  A special convex cutter performs the final cut in both septum and shield plates.  Close fit in the clamshell insures accurate location of CB tube.  Allowable stack-up tolerance for this machining process, and for plate flatness and vacuum pipe geometrical tolerances, depends on beam emittance. Pole design is based on field uniformity requirement.  The ELS pole has no square faces (Fig. 3).  Porches from steel laminations shield the CB from local fringe field, and intercept any stray field away from the CB.  A field clamp bolts to CB tube and to the porches; this reacts vacuum load on the chamber from the upstream ER bellows.
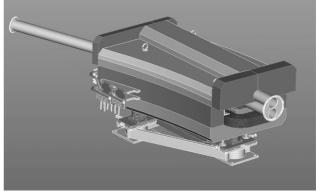


Figure 12: ELS magnet assembly view looking downstream.

## REFERENCES

[1]  C. Pai, et. al.,  "Mechanical Design of Fast Extraction Kicker and PFN for SNS Accumulator Ring", these proceedings.
[2]  Jack   Tanabe,   SLAC,   <u>Accelerator   Magnet Engineering</u>, USPAS 2000.